Numerical Methods in Civil Engineering, 9-1 (2024) 93-102

Numerical Methods in Civil Engineering

Journal Homepage: https://nmce.kntu.ac.ir/

Sufficiency evaluation of ductility requirements of seismic design codes

Reza Fathi[*], Seyed Mehdi Kia[**], Meisam Qorbani-Fouladi[***]

ARTICLE INFO

RESEARCH PAPER

Article history:
Received:
December 2023
Revised:
May 2024
Accepted:
July 2024

Keywords:
Force-reduction factor, Nonlinear Static Analysis, Prescriptive Requirements, Ductility Capacity, Seismic Design Codes

Abstract:

The seismic design philosophy is based on the principle that destructive earthquakes have a low probability of occurrence, and it is not economical to design structures to behave elastically during such rare events. Therefore structures are designed and constructed with much less strength than their elastic demand imposed by destructive earthquakes. This leads to nonlinear deformations and thus damage to structures. However, avoiding collapse damage state requires that structures are able to withstand such large deformations without any significant reduction in the strength and stiffness. This characteristic is known as the ductility capacity of a structure. Since ductility capacity, in the design procedure, is only addressed by satisfying some prescriptive requirements of seismic codes, the fundamental question is: do these provisions ensure adequate ductility capacity to avoid collapse during a destructive earthquake? The answer to this question is the cornerstone of our study. To this end, the present study examines three intermediate steel moment frames of 4, 5, and 7 stories designed according to Iran's national building regulations. Next, the lateral yield strength and ductility capacity of the designed buildings are estimated by performing a nonlinear pushover analysis. Then by developing a set of destructive earthquakes, the maximum elastic lateral strength demand is estimated under each selected earthquakes. The force-reduction factor which is defined as a ratio of the maximum elastic strength demand to the actual lateral yield strength of the structures is then computed. According to the computed force-reduction factors, ductility demands imposed by each of the selected destructive earthquakes are calculated. The obtained ductility demands are next compared with ductility capacity to compute the failure probability of the designed structures during destructive earthquakes. Failure probability is defined as the probability that ductility demand caused by destructive earthquakes will exceed the ductility capacity of structures. Results demonstrate that 4 and 7-story structures have an average failure probability of 30% and 15% under destructive earthquakes respectively. This value of failure probability addresses that there is a lack of proportionality between reduction in the seismic elastic demand and ductility capacity supplied using seismic design requirements, especially in low-rise structures.

1. Introduction

Among the various loads imposed on a structure, the seismic load stands out as one of the most challenging ones. This is mainly due to lack of knowledge about the intensity, duration, and frequency content of earthquakes that occur throughout the structure's lifetime. To overcome this difficulty, the acceleration response spectrum is in seismic design codes to quantify ground motion effects. Using the acceleration response spectrum, the maximum acceleration that a structure with specific dynamic characteristics may experience during a destructive earthquake is estimated. Subsequently, by applying Newton's second law, the maximum lateral elastic force would be computed. Designing structural elements for such a large lateral force is not economically feasible. Therefore, seismic regulations design structures for a lateral force that is significantly less than the maximum lateral elastic force imposed by destructive earthquakes. This causes structures to perform non-linearly during destructive earthquakes, which in turn

[*] *BSc Student in civil Engineering, University of Science and Technology of Mazandaran, Behshahr, Iran. E-mail: reza_fathi@mazust.ac.ir*
[**] *Corresponding author: Assistant Professor, Department of Civil Engineering, University of Science and Technology of Mazandaran, Behshahr, Iran. E-mail:* mehdikia@mazust.ac.ir
[***] *Assistant Professor, Department of Civil Engineering, University of Science and Technology of Mazandaran, Behshahr, Iran. E-mail:* m.qorbani@mazust.ac.ir

https://doi.org/1061186/NMCE.2312.1043

leads to damage to the structures. However, collapse prevention dictates that structures must be able to withstand such nonlinear deformations without losing their strength and stiffness. This capability of structures is known as ductility capacity. Indeed, there should be a tradeoff between the ductility capacity of structures and reduction in the lateral elastic force. Since in the seismic design codes, ductility is only implicitly considered by satisfying a set of code prescriptive requirements, an important question is whether ductility supplied based on these requirements is sufficient for collapse prevention during severe earthquakes? In other words, is there proportionality between the force-reduction factor (R_μ) and ductility demand (μ) imposed by destructive earthquakes. R_μ is defined as the ratio of the elastic strength demand to the actual yield strength of a structure. In addition, μ is usually expressed as a ratio of the maximum deformation observed during earthquake excitation to the actual yield deformation. The answer to this question involves deriving relation between R_μ and μ. As a pioneering and well-known study in this field, Newmark and Hall [1] proposed two approximate relationships between R_μ and μ in terms of the structural period. They have found that for moderate to long-period structures the maximum displacement of elastic and inelastic systems remain within the same range, and for short-period structures the maximum elastic energy and the maximum inelastic energy absorbed by the structures remain within the same range. The first one is known as the Equal Displacement Rule (Figure 1-a) and the latter is recognized as the Equal Energy Rule (Figure 1-b) [2]. Subsequent studies have indicated that the structural hysteretic behavior, fundamental period of structure, soil type, and selected earthquake play an important role in explaining the relationship between R_μ and μ. Therefore, next generation of relationships between R_μ and μ were developed [3–7]. In addition, some other studies were conducted to generalize proposed relationships for multi-degree-of-freedom structures [8],[9]. These investigations aimed to develop modification coefficients while maintaining the framework of the proposed relationships for SDOF.

In the case of more redundant structures, specifically multi-story frames, the redundancy will result in the structure yielding progressively before it reaches its ultimate strength (Figure 1-c). Therefore, a new definition of force-reduction factor which is computed by multiplying R_μ and structural over-strength coefficient (Ω_0) was presented and called Response Modification Factor, R. The evaluation of this quantity is the subject of many previous studies [10-18]. These studies, by computing the R factor, have tried to indirectly address the nonlinear capacity of different structural systems designed according to the seismic codes provisions. However, none of them has answered the question of whether the nonlinear capacity of structural systems reflecting ductility capacity is sufficient to cover ductility demand during destructive earthquakes. The answer to this important gap in previous studies encompasses the central topic and the primary objective of this study.

1. Analytical Models

According to Iran's national building regulations, three intermediate steel moment frames with 4, 5, and 7 stories were designed. The first story of all designed buildings is 2.8 m high and the height of the remaining stories is 3.2 m. Five and seven-story buildings have a rectangular plan with 22 meters in length and 16 meters in width. the four-story building, on the other hand, has a 20 m long square plan. Two perimeter steel moment frames in each direction along with composite steel deck floors are employed to carry lateral and gravity loads, respectively (Figure 2). Beam and column geometries are shown in Table 1. In addition, the fundamental period of 4,5 and 7- story building is 0.74, 0.88, and 1.065 seconds, respectively.

Since the models take advantage of the building's regularity, two-dimensional analytical models are developed in OpenSees software to predict nonlinear structural behavior under seismic loading in each direction. The leaning column concept is also introduced to account for the effect of the gravity load system during nonlinear dynamic analysis. The concentrated plasticity concept is utilized to model the nonlinear behavior of the designed buildings. For this purpose, elastic beam-column elements accompanied by nonlinear rotational springs at both ends *are adopted to* model members' nonlinearity in OpenSees software (Mazzoni et al. 2006 [19]). The mentioned technique of modeling nonlinearity requires the moment of inertia of the elastic-beam column element to be modified so that in combination with the elastic stiffness of the end rotational spring provides the original beam rotational stiffness.

The hysteretic behavior of rotational springs is modeled using Bilin material available in the OpenSees library (Figure 3). The parameters of Bilin material are calculated based on data provided in [20]. In addition, Basic strength, post-capping strength, and unloading stiffness deterioration modes are considered in the formulation of this material according to Rahnama and Krawinkler deterioration rule [3].

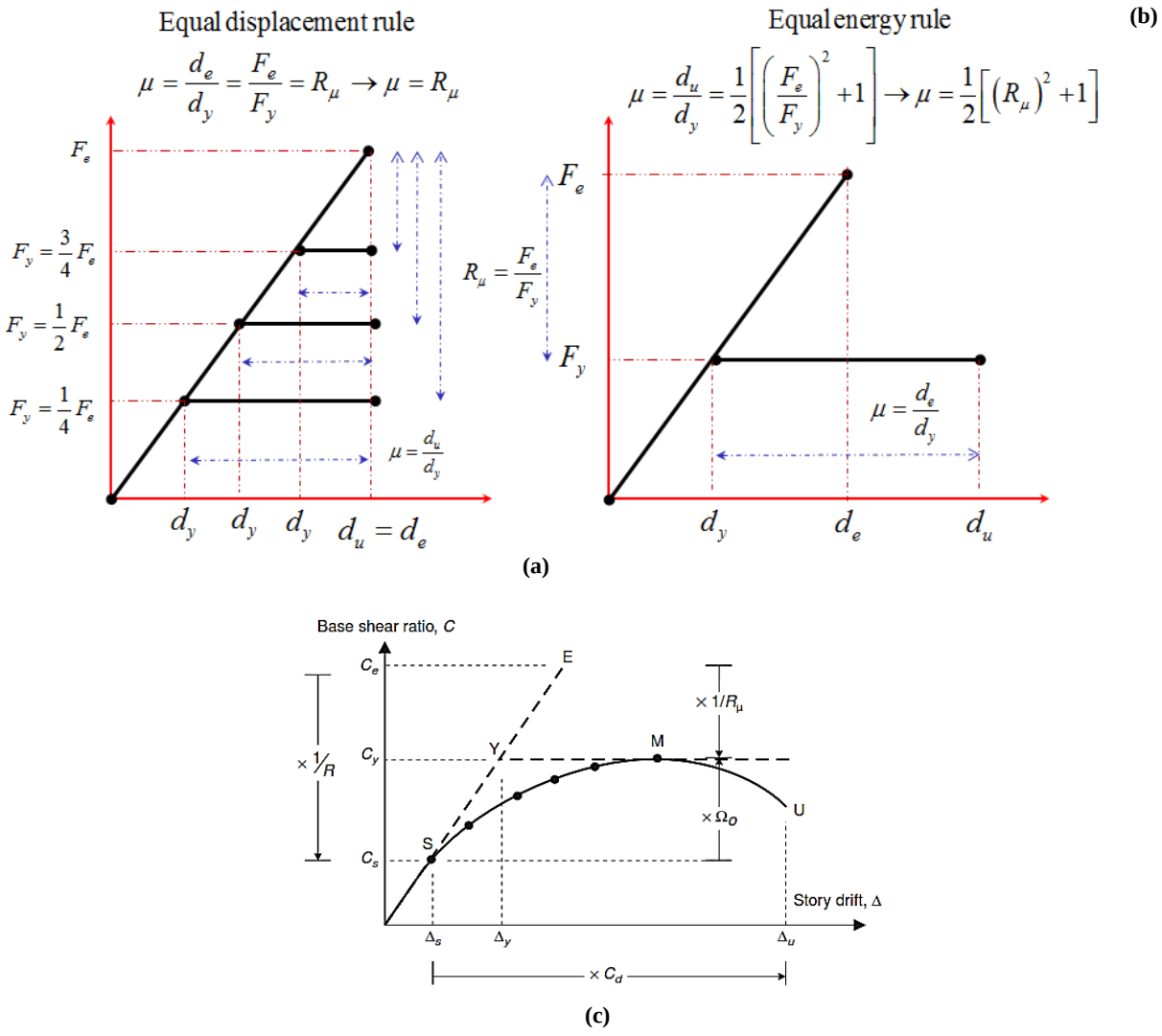

Fig. 1: (a) Equivalent Displacement Rule, (b) Equivalent Energy Rule, (c) Seismic performance factors

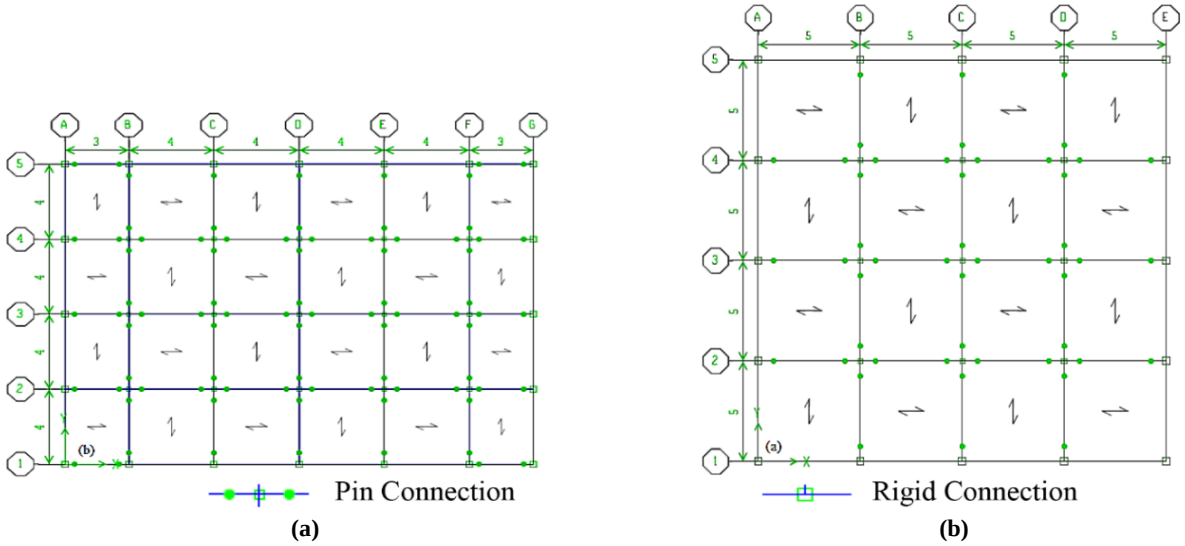

Fig. 2: Plans of Modeled Structures: (a) 4-Story Building Plan (b) Plans for 5 and 7-Story Buildings

Table 1: Beam and Column Sectional Properties

STORY	4 Story-Building		5 Story-Building		7 Story-Building	
	Beam-section	Column-section	Beam-section	Column-section	Beam-section	Column-section
1	IPE450	TUBE 400x400x12	IPE450	TUBE 350x350x12	IPE550	TUBE 400x400x15
2	IPE450	TUBE 400x400x12	IPE450	TUBE 350x350x12	IPE550	TUBE 400x400x15
3	IPE400	TUBE 350x350x12	IPE450	TUBE 350x350x12	IPE550	TUBE 400x400x15
4	IPE400	TUBE 350x350x12	IPE330	TUBE 300x300x12	IPE500	TUBE 400x400x12
5	----	----	IPE330	TUBE 300x300x12	IPE500	TUBE 400x400x12
6	----	----	----	----	IPE400	TUBE 350x350x12
7	----	----	----	----	IPE400	TUBE 350x350x12

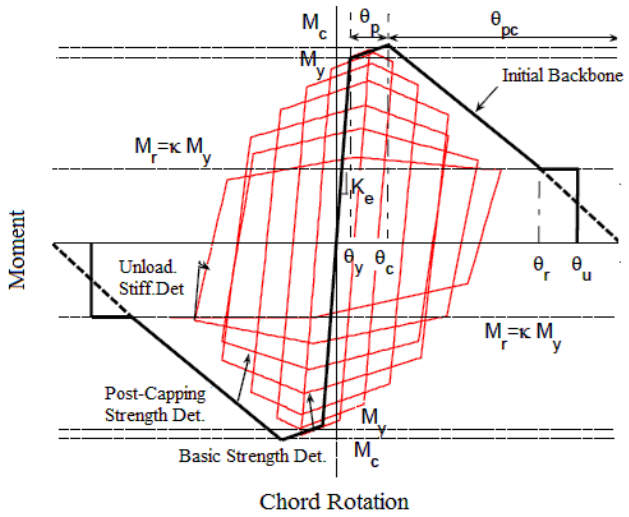

Fig. 3: Bilin-Material Behavioral Model

Rayleigh damping matrix (defined as a linear combination of the mass matrix and stiffness matrix) is computed using 2% of the critical damping applied in the 1st and vibration mode corresponding to 90% of the modal mass of the system. To properly model damping of structures, stiffness proportional damping is applied only to the frame elements and not to the highly rigid truss elements that link the frame and leaning column, nor to the leaning column itself. In addition, zero-length elements have no contribution to the stiffness proportional damping. Furthermore, according to *the appendix of the study conducted by Zareian and* Krawinkler (2006) [21], the stiffness proportional damping coefficient shall be modified due to the modifying moment of inertia of the frame elements. It is worth noting that the five-story structure does not meet the maximum allowable drift restriction. The purpose was to consider a scenario in which the structure lacks adequate lateral stiffness.

3. Ground Motion Records Selection

Simulating structural behavior under destructive earthquakes requires an appropriate set of ground motion records. This is one of the most challenging stages in seismic design. As a general rule, the ground motion records should be unbiased to any site-specific seismological characteristic of a probable future earthquake event. In addition, the number of records in the bin should be enough to cover record-to–record variability in a justified way. According to the mentioned objectives, the general far-field ground motions set originally introduced by FEMA-P695 [22] is used. This set includes 30 pairs of horizontal ground motions, taken from 13 strong seismic events, recorded at sites with soil shear wave velocity greater than 180 m/sec and smaller than 375, and located at a distance 10 to 70 km from fault rupture. This paper defines source-to-site distance as the average of Campbell and Joyner-Boore fault distances provided in the PEER NGA database. All selected motions were recorded in free-field or on the ground floor of a small building to avoid potential soil structure interaction bias in the records set. The magnitudes of the selected seismic events are 6.5 Richter or greater. An earthquake of this magnitude has a relatively long duration and represents a significant amount of energy, causing structural and non-structural damage to engineering structures over a wide area. Furthermore, to avoid potential event-based bias in the ground motion bin, a maximum of six records are allowed to be taken from a single seismic event [22]. In addition, between different ground motions recorded for a single seismic event, only those that have a Peak Ground Acceleration and velocity greater than 0.2 g and 15 cm/sec

are selected. To ensure that low-frequency content is not neglected during the recording process, only records from earthquakes recorded by instruments with a frequency content of at least $Low\ Pass\ Frequency \leq 0.2$ were considered. The complete list of selected records, along with information regarding the year of occurrence, fault mechanism, recording station, and distance from the seismic source, is provided in the appendices (Table A-1).

4. Nonlinear Static Analysis

The nonlinear static analysis, also known as pushover analysis, is one of the most widely used methods to evaluate the performance of a structure under lateral loads. The output of the analysis is a capacity curve. The lateral yield strength and ductility coefficient of a structure can be estimated using a capacity curve. To this end, the capacity curve is substituted with a simple multi-linear force-displacement model. Various methods for idealizing pushover curves have been proposed in technical texts, including those recommended in ATC-19 [23], Paulay and Priestley [24], ATC-40 [25], and FEMA 356 [26]. Figure 4 illustrates each of these methods graphically.

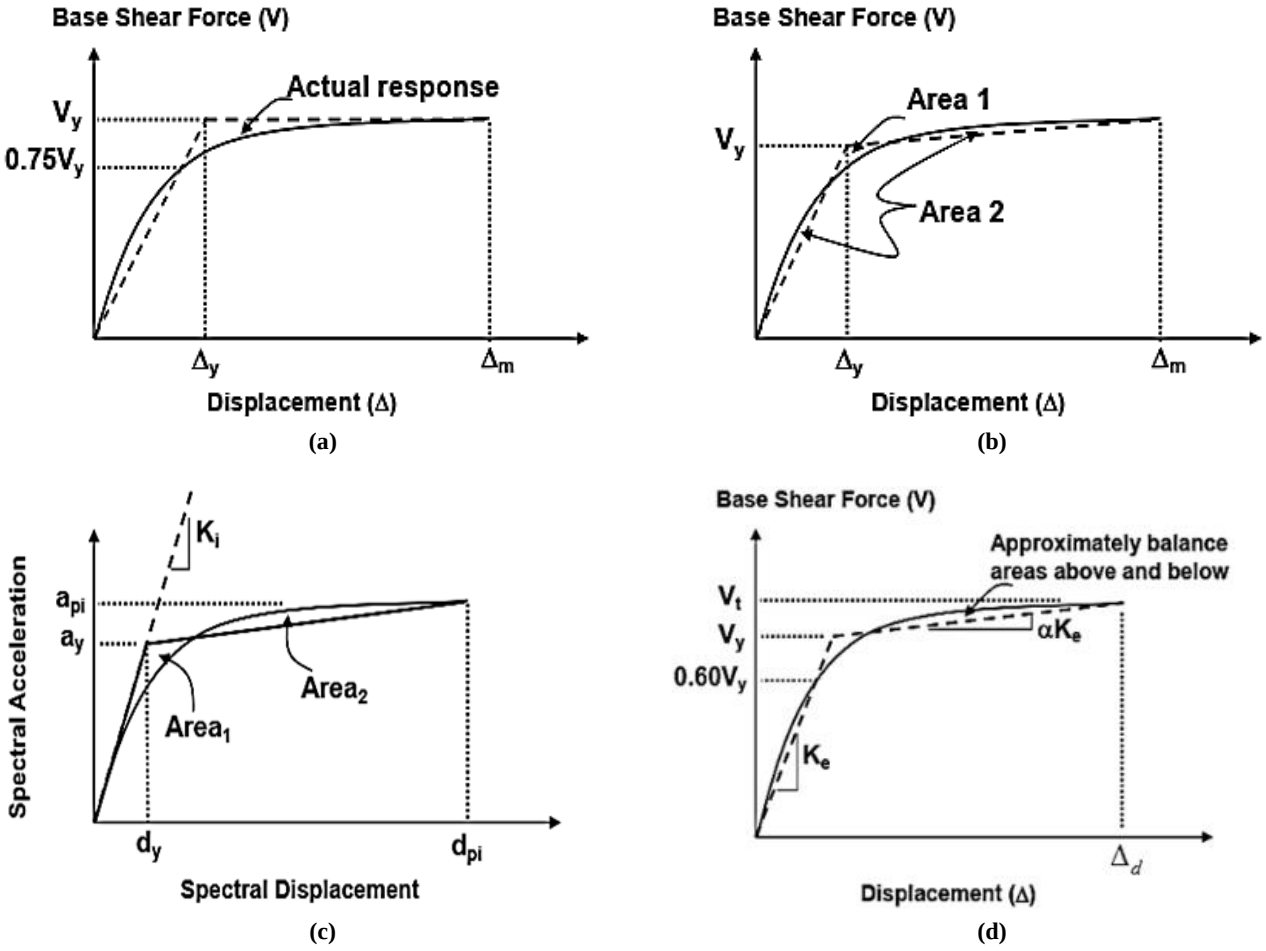

Fig. 4: Idealization of the Structural Capacity Curve a) Paulay & Piestly b) ATC-19 c) ATC-40 d) FEMA 365
(Note: K_i = Initial Stiffness, $Area_1 \cong Area_2$)

In this paper, the proposed FEMA 356 method has been employed. In this method, the first segment of the simplified multi-linear model is drawn in a way that passes through the point $0.6\ V_y$. In the simplified model, it must be ensured that V_y is not greater than the maximum base shear in the capacity curve. The second line, with a positive slope, is drawn by utilizing the points $(V_t, \Delta_d), (V_y, \Delta_y)$ and intersecting with the first line in such a way that the area under the two-linear model is equal to the area under the capacity curve up to the point (V_t, Δ_d) . The point (V_t, Δ_d)on the capacity curve defines the displacement corresponding to the maximum shear force. Nevertheless, the aforementioned references provide no recommendations to idealize the capacity curve beyond the point Δ_d . It is worth noting that in the 2014 edition of Instruction for Seismic Rehabilitation of Existing Buildings No 360, it is suggested that the third line, with a

negative slope, should be drawn using the points (V_t, Δ_d) and the point on the capacity curve where the shear force is equal to 0.6 V_y. However, due to numerical instability during analysis, achieving such a displacement level was not feasible. Therefore, the third line with a negative slope was drawn using the point (V_t, Δ_d) and the point where the shear force is equal to V_y, although it does not affect the results. According to above mentioned procedure, the capacity curve and thus the simplified multi-linear model for the studied structures were prepared and presented in Figure 5.
Based on the simplified curves, the values of lateral yield capacity and ductility were calculated and are presented in the Table 2.

Table 2: Lateral Yield Capacity and Ductility Coefficient

Ductility & Yield Strength		
	Yield Strength (Ton)	**Ductility**
4-Story Building	148.00	2.82
5-Story Building	132.00	2.54
7-Story Building	200.00	3.11

5. Calculation of Elastic Demand and Force Reduction Factor

To calculate seismic elastic demand, the acceleration response spectrum of selected earthquakes are extracted using the SeismoSignal software. The spectral acceleration of 4,5 and 7-story buildings is then calculated according to the fundamental period of the structures. Next, multiplying the mass of the structure by the corresponding spectral acceleration is concluded seismic elastic demand, and results are presented in Table 3. The force-reduction factor is computed by dividing the seismic elastic demand by the lateral yield strength.

6. $R_\mu - \mu$ Relationship

Riddell et al [27], by applying inelastic spectra for four sets of earthquakes recorded on stiff and well-consolidated soil, proposed an equation to calculate the ductility reduction coefficient of single-degree-of-freedom (SDOF) systems. The systems had an elastoplastic behavior and a 5% damping ratio. The mathematical expression of the proposed equation is as follows.

$$R_\mu = \frac{R^* - 1}{T^*} T \quad 0 \le T \le T^* \qquad R_\mu = R^* \quad T^* \le T \tag{1}$$

In the above relationship, T represents the structural period, and T* and R* are constants that vary proportionally with the ductility coefficient, ranging between 0.1 to 0.4 and 2 to 8, respectively, as indicated in Table 4. This relationship is applicable for ductility coefficients in the range of 2 to 10.

Table 4: Calculation of T^* & R^* (Riddell and Colleagues' Relationship)

μ	2	3	4	5	6	7	8	9	10
R*	2	3	4	5	5.6	6.2	6.8	7.4	8
T*	0.1	0.2	0.3	0.4	0.4	0.4	0.4	0.4	0.4

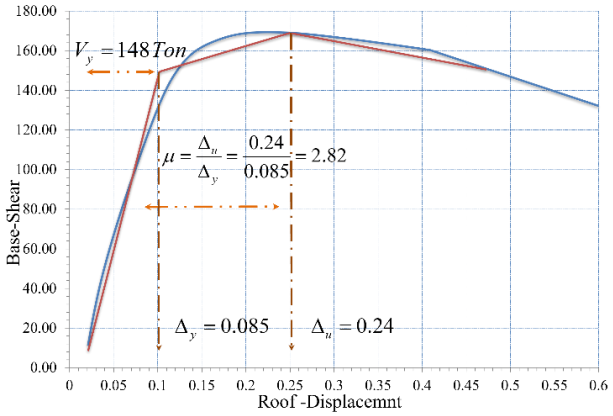

(a)

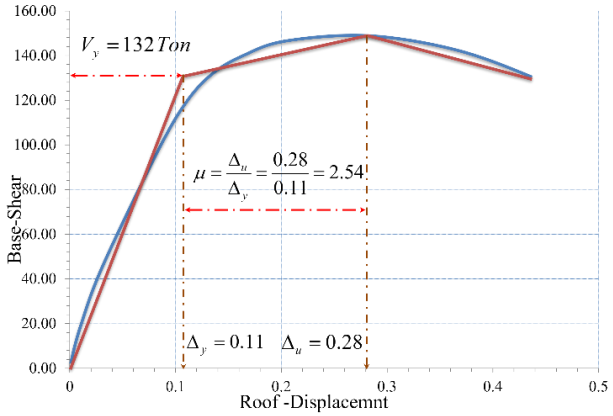

(b)

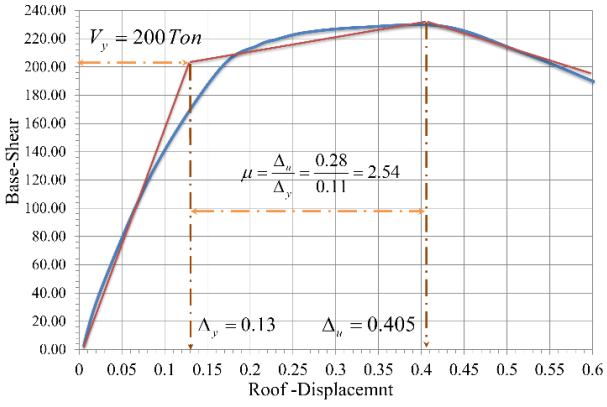

(c)

Fig. 5: (a) Capacity Curve of the 4-story Structure, (b) Capacity Curve of the 5-story Structure, (c) Capacity Curve of the 7-story Structure

Table 3: Seismic Elastic Demand Values and Force-Reduction Factor

Range of $S_a(T)$	4-story			5-story			7-story		
	[1]Count of Record	Range of $V_e(Ton)$	Range of R_μ	[1]Count of Record	Range of $V_e(Ton)$	Range of R_μ	[1]Count of Record	Range of $V_e(Ton)$	Range of R_μ
[0.1 , 0.3)	11	75.68 – 165.59	0.51 – 1.12	16	99.61 – 183.11	0.75 – 1.39	25	90.43 – 250.4	0.45 – 1.25
[0.3 , 0.5)	18	173.39 – 277.33	1.17 – 1.87	22	189.27 – 302.43	1.43 – 2.29	23	262.76 – 418.32	1.31 – 2.09
[0.5 , 0.7)	15	282.41 – 386.97	1.91 – 2.61	14	313.94 – 429.77	2.38 – 3.26	5	434.74 – 546.84	2.17 – 2.73
[0.7 , 0.9)	7	398.16 – 483.78	2.69 – 3.27	1	526.83	3.99	2	616.78 – 638.45	3.08 – 3.19
[0.9 , 1.1)	6	512.27 – 608.23	3.46 – 4.11	-	-	-	4	791.56 – 863.8	3.96 – 4.32
[**1**.1 , 1.3)	-	-	-	3	729.1 -773.99	5.52 – 5.86	-	-	-
[**1**.3 , 1.5)	1	736.98	4.98	2	828.71 – 852.96	6.28 – 6.46	1	1129.28	5.65
[**1**.5 , 1.8)	-	-	-	1	1072.2	8.12	-	-	-
[**1**.8 , 2.06)	2	1030.58 – 1167	6.96 – 7.89	1	1135.62	8.6	-	-	-

[1]-As described in section 3, in this study, a set of 30 pairs of horizontal ground motion records is considered. Since each pair has two horizontal components, the total number of records will be 60.

$Sa(T)$ is defined in terms of gravitional acceleration (e.g. the Sa(T) of record number 1 is 0.66g)

$V_e = W \times Sa$, where W defines seismic weight, and computed as $W_{Dead\_Load} + 0.2W_{Live\_Load}$

Naser and Krawinkler [28] subjected nonlinear single-degree-of-freedom systems to 15 ground motion records. All ground motion excitations are recorded in the western United States. In this study, the sensitivity of the force-reduction factor relative to hypocenter distance and some structural parameters are investigated, and consequently, the following relationships were presented

$$R_\mu = [c(\mu - 1) + 1]^{\frac{1}{c}} \quad (2)$$

$$c(T, \alpha) = \frac{T^a}{1 + T^a} + \frac{b}{T} \quad (3)$$

In Equation 3, α is defined as the ratio of post-yielding stiffness to initial stiffness. In addition, the coefficients a and b are calculated according to Table 5.

Table 5: Calculation of Coefficient Values a and b

α	a	b
0.00	1	0.42
0.02	1	0.37
1	0.8	0.29

Miranda [29,30] investigated the impact of a variety of ground motion characteristics on the force-reduction coefficient. To this end, a set of 124 ground motion excitations is selected and then classified into three categories, including: a) ground motions recorded on bedrock, b) excitations recorded on alluvial soil, and finally ground motions recorded on very soft soil. In the mentioned study, the force-reduction factor of bi-linear single-degree-of-freedom systems with a 5% damping ratio and ductility coefficients between 2 to 6 were investigated. The study concluded that site soil conditions significantly influence the force-reduction factor, but earthquake magnitude and hypocenter distance have a negligible effect on the force-reduction coefficients. Based on this study, the following mathematical expression is presented:

$$R_\mu = \frac{\mu - 1}{\phi} + 1 \geq 1 \quad (4)$$

In the above equation, ϕ is a function of the ductility coefficient, the fundamental period of structure (T), and the site soil conditions. this quantity is calculated using equations (5), (6) and (7):

$$\phi = 1 + \frac{1}{10T - \mu T} - \frac{1}{2T} exp\left[-\frac{3}{2}(ln\, T - \frac{3}{5})^2\right] \quad (5)$$

$$\phi = 1 + \frac{1}{12T - \mu T} - \frac{2}{5T} exp\left[-2(ln\, T - \frac{1}{5})^2\right] \quad (6)$$

$$\phi = 1 + \frac{T_g}{3T} - \frac{3T_g}{4T} exp\left[-3(ln\frac{T}{T_g} - \frac{1}{4})^2\right] \quad (7)$$

In the above equations, T_g represents the characteristic period of the site.

Vidic et al. [8] in 1994, proposed a simple relationship for estimating force-reduction coefficient. In this study, single-degree-of-freedom systems with hysteretic behavior represented by a bi-linear model and stiffness degradation were considered. Based on the results obtained in this study, the following relationship in equations (8) a (9) was presented for a 5% damping ratio:

$$\begin{aligned} R_\mu &= C_1(\mu - 1)^{C_R}(\frac{T}{T_0}) + 1 && T \leq T_0 \\ R_\mu &= C_1(\mu - 1)^{C_R} + 1 && T_0 \leq T \end{aligned} \quad (8)$$

$$T_0 = C_2 \mu^{C_T} T_g \quad (9)$$

In the above equations, T represents the structural period, T_g is the characteristic period of the site, and the coefficients C are calculated based on the type of damping and the structural hysteretic behavior from Table 6.

7. Results

In this section, the ductility demand of three designed structures, according to the value of force-reduction coefficients presented in Table 3, are calculated by equations proposed in the previous section. The results are modified by the following equation to be acceptable for multi-degree-of-freedom systems and then presented in Table 7.

$$R_T = \frac{1}{1 + 0.15T^2 Ln(\mu)} \quad (10)$$

Given the dispersion of the data presented in Table 7, it is essential to apply a probabilistic framework to answer the question "whether ductility capacity is sufficient for collapse prevention during severe earthquakes?" To answer this question, the probability that ductility demand caused by destructive earthquakes will exceed the ductility capacity of structures, i.e. $P(\mu_{demand} > \mu_{capacity})$ is computed using data presented in Table 7. This quantity is named failure probability. Computing failure probability is started by sorting the database from large to small values in a vector. Equation (11) is next applied to calculate failure probability. Results are presented in Table 8.

$$P(\mu_{demand} \geq \mu_{capacity}) = \frac{\text{the number of data greater than or equal to ductility capacity value}}{\text{Total number of data}} \quad (11)$$

Table 6. Coefficients of Equations (8) and (9) corresponding to the structural hysteretic behavior

C_T	C_R	C_2	C_1	**Damping Type**	**Structural hysteretic behaviour**
0.2	0.95	0.75	1.35	mass damping	**Without degradation**
0.2	0.95	0.75	1.1	Stiffness damping	**Without degradation**
0.3	1	0.65	1	mass damping	**With degradation**
0.3	1	0.65	0.75	Stiffness damping	**With degradation**

Table 8: Failure Probability of the Structures

Riddle et al	0.36	0.4	0.17
Nasser et al	0.30	0.38	0.13
Miranda	0.23	0.27	0.12
Vidic et al	0.27	0.28	0.15
Average	0.29	0.36	0.14

Table 7: Ductility demand of 4, 5, and 7-story Structures

Range of Ductility (μ)	**4-Story Building**				**5-Story Building**				**7-Story Building**			
	Riddel et al	**Nassar et al**	**Miranda**	**Vidic et al**	**Riddel et al**	**Nassar et al**	**Miranda**	**Vidic et al**	**Riddel et al**	**Nassar et al**	**Miranda**	**Vidic et al**
[1 , 1.5)	16	17	19	19	13	13	16	13	22	24	30	25
[1.5 , 2)	7	9	11	10	11	12	15	12	15	14	17	13
[2 , 2.5)	9	10	8	7	11	12	8	12	10	11	4	10
[2.5 , 3)	13	11	9	9	6	9	10	7	4	4	2	4
[3 , 3.5)	5	4	3	5	8	6	3	5	2	0	2	1
[3.5 , 4)	5	4	5	5	3	0	1	3	2	2	2	2
[4 , 5)	2	3	2	2	1	1	0	1	2	4	2	3
[5 , 7)	1	1	3	1	0	5	5	3	2	1	1	2
[7 , 10.3)	2	1	0	2	7	2	2	4	1	0	0	0

8. Conclusion

In the present study, the proportionality between the reduction in seismic elastic demand and ductility supplied using prescriptive requirements is evaluated. Therefore, three intermediate steel moment frames with 4, 5, and 7 stories are designed according to the steel structure design code and Standard 2800. Among them, a 5-story building was designed in such a way that the maximum story drift criterion was not met. According to the results of the investigations, the following conclusions can be drawn:

- Seismic design procedure suffers from a lack of proportionality between lateral design forces and

ductility provided by the prescribed requirements in seismic codes. Overcoming this difficulty necessitates increasing lateral design forces or enhancing ductility capacity by rethinking the prescriptive requirements in seismic design codes.

- The probability of failure decreases as the number of floors increases. In other words, taller structures are less likely to collapse than low-to-mid-rise structures. The 4-story structure has an average failure probability of 30% under selected destructive earthquakes, While the average probability of failure of the 7-story building, representing a relatively mid-rise structure in this study, is about 15%, which is significantly lower than the failure probability of the 4-story structure.

- The investigations demonstrate that the lack of lateral rigidity diminishes the effectiveness of seismic design provisions in ensuring adequate ductility. This increases the probability of structural failure (refer to the structure of five stories).

9. References

[1] Newmark, N. M., and Hall, W. J. 1982. Earthquake Spectra and Design. Berkeley, CA: EERI.

[2] Porcu, M. C., Vielma Pérez, J. C., Pais, G., Osorio Bravo, D., & Vielma Quintero, J. C. (2022). Some issues in the seismic assessment of shear-wall buildings through code-compliant dynamic analyses. Buildings, 12(5), 694.

[3] Rahnama, M., & Krawinkler, H. (1994). Effects of P-delta and Strength Deterioration on SDOF Strength Demands. In Proceedings of the 10th European Conference in Earthquake Engineering, Vienna, Austria.

[4] Lee, L. H., Han, S. W., & Oh, Y. H. (1999). Determination of ductility factor considering different hysteretic models. Earthquake engineering & structural dynamics, 28(9), 957-977.

[5] Fajfar, P., Vidic, T., & Fischinger, M. (1989). Seismic demand in medium-and long-period structures. Earthquake Engineering & Structural Dynamics, 18(8), 1133-1144.

[6] Rahnama-Hazaveh, M. (1993). Effects of soft soil and hysteresis model on seismic demands (Doctoral dissertation, Stanford University).

[7] Fischinger, M., Fajfar, P., & Vidic, T. (1994). Factors contributing to the response reduction.

[8] Vidic, T., Fajfar, P., & Fischinger, M. (1994). Consistent inelastic design spectra: strength and displacement. Earthquake Engineering & Structural Dynamics, 23(5), 507-521.

[9] Nassar, A. A., Osteraas, J. D., & Krawinkler, H. (1992, July). Seismic design based on strength and ductility demands. In 10th world conference on earthquake engineering (Vol. 10, pp. 5861-5866).

[10] Aliakbari, F., & Shariatmadar, H. (2019). Seismic response modification factor for steel slit panel-frames. *Engineering Structures*, *181*, 427-436.

[11] Fanaie, N., & Shamlou, S. O. (2015). Response modification factor of mixed structures. *Steel and Composite Structures*, *19*(6), 1449-1466.

[12] Güner, T., & Topkaya, C. (2020). Performance comparison of BRBFs designed using different response modification factors. *Engineering Structures*, *225*, 111281.

[13] Asgarian, B., & Shokrgozar, H. R. (2009). BRBF response modification factor. *Journal of constructional steel research*, *65*(2), 290-298.

[14] Sohrabi-Haghighat, M., & Ashtari, P. (2019). Evaluation of seismic performance factors for high-rise steel structures with diagrid system. *KSCE Journal of Civil Engineering*, *23*(11), 4718-4726.

[15] Mohsenian, V., Padashpour, S., & Hajirasouliha, I. (2020). Seismic reliability analysis and estimation of multilevel response modification factor for steel diagrid structural systems. *Journal of Building Engineering*, *29*, 101168.

[16] Kim, J., & Choi, H. (2005). Response modification factors of chevron-braced frames. *Engineering structures*, *27*(2), 285-300.

[17] Mohsenian, V., Hajirasouliha, I., & Nikkhoo, A. (2022). Multi-level response modification factor estimation for steel moment-resisting frames using endurance-time method. *Journal of Earthquake Engineering*, *26*(9), 4812-4832.

[18] Abdi, H., Hejazi, F., Saifulnaz, R., Karim, I. A., & Jaafar, M. S. (2015). Response modification factor for steel structure equipped with viscous damper device. *International Journal of Steel Structures*, *15*, 605-622.

[19] Mazzoni, S., McKenna, F., Scott, M. H., & Fenves, G. L. (2006). OpenSees command language manual. *Pacific earthquake engineering research (PEER) center*, *264*(1), 137-158.

[20] Lignos, D. G., & Krawinkler, H. (2012). Sideway Collapse of deteriorating structural system under seismic excitations", Report 177 (Doctoral dissertation, Ph. D. diss., John A. Blume Earthquake Engineering Center, Stanford University).

[21] Zareian, F. (2006). *Simplified performance-based earthquake engineering*. Stanford University.

[22] Applied Technology Council. (2009). Quantification of building seismic performance factors. US Department of Homeland Security, FEMA.

[23] Applied Technology Council, ATC-19, 1995, Structural Response Modification Factors, Redwood City, California.

[24] Paulay, T., & Priestley, M. N. (1992). Seismic design of reinforced concrete and masonry buildings (Vol. 768). New York: Wiley.

[25] ATC, S. (1996). Evaluation and retrofit of concrete buildings, Rep. ATC-40, Applied Technology Council, Redwood City, California.

[26] Prestandard, F. E. M. A. (2000). Commentary for the seismic rehabilitation of buildings (FEMA356). Washington, DC: Federal Emergency Management Agency, 7(2).

[27] Riddell, R., Hidalgo, P., & Cruz, E. (1989). Response modification factors for earthquake resistant design of short period buildings. Earthquake spectra, 5(3), 571-590.

[28] Nassar, A.A, and Krawinkler, H., "Seismic Demands for SDOF and MDOF systems," Report No. 95, The John A. Blume Earthquake Engineering Center, Stanford University, Stanford, California, 1991

[29] Miranda, E. (1993). Site-dependent strength-reduction factors. Journal of Structural Engineering, 119(12), 3503-3519.

[30] Miranda, E. (1997, January). Strength reduction factors in performance-based design. In Proceedings of EERC-CUREe Symposium, Berkeley, CA.

Appendix

Table A-1: Information of Used Record

			Event Information				Site Information				Record Information
EQ Index	**EQ ID**	**PEER-NGA Rec. Num**	**Mag.**	**Year**	**Event**	**Fault Type**	**Station Name**	**Vs_30 (m/s)**	**Campbell Distance**	**Joyner-Boore**	**Lowest Useable Freq. (Hz)**
1	12011	953	6.7	1994	Northridge	Blind thrust	Beverly Hills - 14145 Mulhol	356	17.2	9.4	0.25
2	12012	960	6.7	1994	Northridge	Blind thrust	Canyon Country - W Lost Cany	309	12.4	11.4	0.13
3	12013	1003	6.7	1994	Northridge	Blind thrust	LA - Saturn St	309	27.0	21.2	0.13
4	12014	1077	6.7	1994	Northridge	Blind thrust	Santa Monica City Hall	336	27.0	17.3	0.14
5	12041	1602	7.1	1999	Duzce,Turkey	Strike-slip	Bolu	326	12.4	12.0	0.06
6	12061	169	6.5	1979	Imperial Valley	Strike-slip	Delta	275	22.5	22.0	0.06
7	12062	174	6.5	1979	Imperial Valley	Strike-slip	El Centro Array #11	196	13.5	12.5	0.25
8	12063	162	6.5	1979	Imperial Valley	Strike-slip	Calexico Fire Station	231	11.6	10.5	0.25
9	12064	189	6.5	1979	Imperial Valley	Strike-slip	SAHOP Casa Flores	339	10.8	9.6	0.25
10	12072	1116	6.9	1995	Kobe, Japan	Strike-slip	Shin-Osaka	256	28.5	19.1	0.13
11	12073	1107	6.9	1995	Kobe, Japan	Strike-slip	Kakogawa	312	3.2	22.5	0.13
12	12074	1106	6.9	1995	Kobe, Japan	Strike-slip	KJMA	312	95.8	0.9	0.06
13	12081	1158	7.5	1999	Kocaeli,Turkey	Strike-slip	Duzce	276	15.4	13.6	0.24
14	12091	900	7.3	1992	Landers	Strike-slip	Yermo Fire Station	354	23.8	23.6	0.07
15	12092	848	7.3	1992	Landers	Strike-slip	Coolwater	271	20.0	19.7	0.13
16	12101	752	6.9	1989	Loma Prieta	Strike-slip	Capitola	289	35.5	8.7	0.13
17	12102	767	6.9	1989	Loma Prieta	Strike-slip	Gilroy Array #3	350	12.8	12.2	0.13
18	12103	783	6.9	1989	Loma Prieta	Strike-slip	Oakland - Outer Harbor Wharf	249	74.3	74.2	0.13
19	12104	776	6.9	1989	Loma Prieta	Strike-slip	Hollister - South & Pine	371	27.9	27.7	0.13
20	12105	777	6.9	1989	Loma Prieta	Strike-slip	Hollister City Hall	199	27.6	27.4	0.13
21	12106	778	6.9	1989	Loma Prieta	Strike-slip	Hollister Diff. Array	216	24.8	24.5	0.13
22	12121	721	6.5	1987	Superstition Hills	Strike-slip	El Centro Imp. Co. Cent	192	18.5	18.2	0.13
23	12122	725	6.5	1987	Superstition Hills	Strike-slip	Poe Road (temp)	208	11.7	11.2	0.25
24	12123	728	6.5	1987	Superstition Hills	Strike-slip	Westmorland Fire Sta	194	13.5	13.0	0.13
25	12132	829	7.0	1992	Cape Mendocino	Thrust	Rio Dell Overpass - FF	312	14.3	7.9	0.07
26	12141	1244	7.6	1999	Chi-Chi, Taiwan	Thrust	CHY101	259	15.5	10.0	0.05
27	12145	1595	7.6	1999	Chi-Chi, Taiwan	Thrust	WGK	259	15.4	10.0	0.09
28	12151	68	6.6	1971	San Fernando	Thrust	LA - Hollywood Stor FF	316	25.9	22.8	0.25
29	12053	1762	7.1	1999	Hector Mine	Strike-slip	CDMG 21081 Amboy	271.4	43.05	41.82	0.08
30		138	7.4	1978	Tabas, Iran	Thrust	70 Boshrooyeh	338.6	28.79	24.07	0.16